Theoretical and Applied Climatology (2020) 140:167–182
https://doi.org/10.1007/s00704-019-03081-7

ORIGINAL PAPER

Assessing the impact of climate changes on the potential yields of maize and paddy rice in Northeast China by 2050

Luoman Pu[1,2,3] · Shuwen Zhang[2] · Jiuchun Yang[2] · Liping Chang[2] · Xiangming Xiao[3]

Received: 21 August 2019 / Accepted: 19 December 2019 / Published online: 3 January 2020

Abstract

Northeast China is the main crop production region in China, and future climate change will directly impact crop potential yields, so exploring crop potential yields under future climate scenarios in Northeast China is extremely critical for ensuring future food security. Here, this study projected the climate changes using 12 general circulation models (GCMs) under two moderate Representative Concentration Pathway (RCP) scenarios (RCP 4.5 and 6.0) from 2015 to 2050. Then, based on the Global Agro-ecological Zones (GAEZ) model, we explored the effect of climate change on the potential yields of maize and paddy rice in Northeast China during 2015–2050. The annual relative humidity increased almost throughout the Northeast China under two RCPs. The annual precipitation increased more than 400 mm in some west, east, and south areas under RCP 4.5, but decreased slightly in some areas under RCP 6.0. The annual wind speed increased over 2 m/s in the west region. The annual net solar radiation changes varied significantly with latitude, but the changes of annual maximum temperature and minimum temperature were closely related to the terrain. Under RCP 4.5, the average maize potential yield increased by 34.31% under the influence of climate changes from 2015 to 2050. The average rice potential yield increased by 16.82% from 2015 to 2050. Under RCP 6.0, the average maize and rice potential yields increased by 25.65% and 6.34% respectively. The changes of maize potential yields were positively correlated with the changes of precipitation, wind speed, and net solar radiation (the correlation coefficients were > 0.2), and negatively correlated with the changes of relative humidity, minimum and maximum temperature under two RCPs. The changes of rice potential yields were positively correlated with the changes of precipitation (correlation coefficient = 0.15) under RCP 4.5. Under RCP 6.0, it had a slight positive correlation with net solar radiation, relative humidity, and wind speed.

1 Introduction

Global concentrations of greenhouse gases (GHG) in the atmosphere have significantly increased since the pre-industrial era (Miao et al. 2013), and anthropogenic emissions of greenhouse gases are constantly changing the earth's climate (Araya et al. 2015). It is expected to lead to increasing sea level and temperatures, reducing near-surface permafrost extent, changes in rainfall regimes, and increasing extreme weather events (Padgham 2009; Solomon et al. 2007). The general circulation models (GCMs) included in the Coupled Model Intercomparison Project Phase 5 (CMIP5) have been generated and can be used to simulate history and future climate conditions (Zhou and Wang 2015). The Representative Concentration Pathways (RCPs) describe four different twenty-first century pathways of GHG emissions, including a very slight GHG emission scenario (RCP2.6), two intermediate scenarios (RCP4.5 and RCP6.0), and one very high GHG emission scenario (RCP8.5). The four RCPs indicate that the increase of global mean surface temperature is *likely* to be 0.3 to 1.7 °C under RCP2.6, 1.1 to 2.6 °C under RCP4.5, 1.4 to 3.1 °C under RCP6.0, and 2.6 to 4.8 °C under RCP8.5 by the end of the twenty-first century (2081–2100) relative to 1986–2005 (Pachauri et al. 2014).

Climate change and the potential impact on society are enormous challenges for mankind, and agriculture is one of the most sensitive sectors to climate change (Zhou and Wang

✉ Shuwen Zhang
zhangshuwen@neigae.ac.cn

[1] College of Earth Sciences, Jilin University, Changchun 130012, China

[2] Northeast Institute of Geography and Agroecology, Chinese Academy of Sciences, Changchun 130102, China

[3] Department of Microbiology and Plant Biology, Center for Spatial Analysis, University of Oklahoma, Norman, OK 73019, USA

2015). Climate change will substantially affect productivity of major staple food crops such as maize and rice (Bassu et al. 2014 ; Jones and Thornton 2003; Ruane et al. 2013; Tao and Zhang 2010) because growth and development of crops are mainly dependent on sunlight, temperature, and water (Chen et al. 2013). On the one hand, global warming could alter the dynamics and intensity of crop damage by pests and diseases, such as insects and plant pathogens (Cannon 1998; Scherm 2004). On the other hand, a higher atmospheric concentration of carbon dioxide can improve photosynthesis, enhance biomass accumulation, and increase production (Schmidhuber and Tubiello 2007). Therefore, the impact of climate change on crop yield is positive in some agricultural regions and negative in others (Parry et al. 2004).

Maize, soybean, wheat, and paddy rice are major crops in Northeast China, and maize has the largest planting area and production among the three dryland crops. The climate changes can affect crop phenology, growth, and yield, and threaten sustainable crop production in Northeast China in the future. Some studies applied the GCMs to analyze the future climate changes and evaluate the impact of climate changes on crop growth, but most studies rely on only a few climate models or one GHG emission scenario, which were unable to guarantee the accuracy and rationality of climate predicted results (Kassie et al. 2015; Lu et al. 2018; Meehl et al. 2007; Tao et al. 2009; Zhou and Wang 2015). For example, Kassie et al. (2015) only used three GCMs, including CanESM2, HadGEM2-ES, and CSIRO-MK3-6-0 to explore climate change impacts and adaptation options for maize production in the Central Rift Valley of Ethiopia. Lu et al. (2018) also used three GCMs to study the spatial difference characteristics on simulation capability of seasonal variation of air temperature. Although Zhou and Wang (2015) applied 30 GCMs to analyze the potential impact of future climate change on single-rice and spring-maize yields in Northeast China, they only considered the RCP 4.5 scenario. More robust and precise climate change impact assessment studies are based on different GCM projections and multiple RCPs (Araya et al. 2015, 2017; Tebaldi and Knutti 2007). For instance, Araya et al. (2015) assessed the impact of climate changes on maize yield using climate simulation results from 20 different GCMs under high and moderate RCP scenarios in southwestern Ethiopia. After 2 years, they assessed the impact of climate changes on maize productivity during 2040–2069 in relation to the baseline (1980–2009) in Kansas using 20 GCMs and two RCPs. In assessing the crop potential yields, the best option is to apply process-based crop models, which emphasize physiological processes of crop growth, such as the Environmental Policy Integrated Climate (EPIC) model (Izaurralde et al. 2006; Williams et al. 1989) and World Food Studies (WOFOST) model (Diepen et al. 2010). Crop models derived yield predictions based on multiple GCMs and RCPs can provide more reliable climate change impact assessments (Asseng 2013; Ruane et al. 2013). Therefore, the highlight of this study is to combine 12 GCMs with the process-based crop model, Global Agricultural Ecological Zones (GAEZ) model, to predict future climate and explore the impact of climate changes on maize and paddy rice yields in Northeast China. Because the moderate emission scenarios were more suitable for China's sustainable development pattern in the future, the two moderate emission scenarios, RCP 4.5 and 6.0, were considered in this study.

Therefore, the objectives of this study were to (1) project the climate of Northeast China in 2050 based on 12 different GCMs under two moderate RCPs, RCP 4.5 and 6.0; (2) simulate the potential yields of maize and paddy rice in base year (2015) and future year (2050) using the GAEZ model, and analyze the maize and rice potential yield changes during 2015–2050; and (3) explore the impact of future climate changes on the potential yields of maize and paddy rice. Assessing crop potential yield changes resulting from future climate changes is critical to supply policy makers with information to develop appropriate plans in order to reduce the negative impacts of climate changes and improve the ability of agricultural systems to meet future food demand and ensure food security (Lv et al. 2015).

2 Data and methods

2.1 Study area

Northeast China covers Heilongjiang, Jilin, Liaoning, and the eastern parts of the Inner Mongolia Autonomous Region (IMAR), extending from 38° 40′ N to 53° 34′ N, and 115° 05′ E to 135° 02′ E (Fig. 1). Total land area of Northeast China is about 1.24 million km^2. It is surrounded by many middle and low mountains, such as the Changbai Mountains in the southeast, the Greater Khingan Mountains in the northwest, and the Lesser Khingan Mountains in the northeast (Mao et al. 2012). Three major plains are located in northeast China, including the Sanjiang Plain in the northeastern corner, Songnen Plain in the central part, and Liaohe Plain in the southern part. The climate is influenced by the East Asian monsoon, which has four distinct seasons, with a long winter and a short summer (Gao et al. 2018). The annual temperature ranges from − 5 to 10.6 °C with the spatial increase from north to south and ≥ 10 °C annual accumulated temperature is 2200–3600 °C. The frost-free period is 140–170 days (Tan et al. 2014). The average annual precipitation ranges from 1000 mm in the east to 400 mm in the west, which is concentrated from July to September and represents 70% of the annual total. The corresponding main soil types in Northeast China are brown coniferous forest soils in the cold temperate zone, dark brown forest soil in the warm

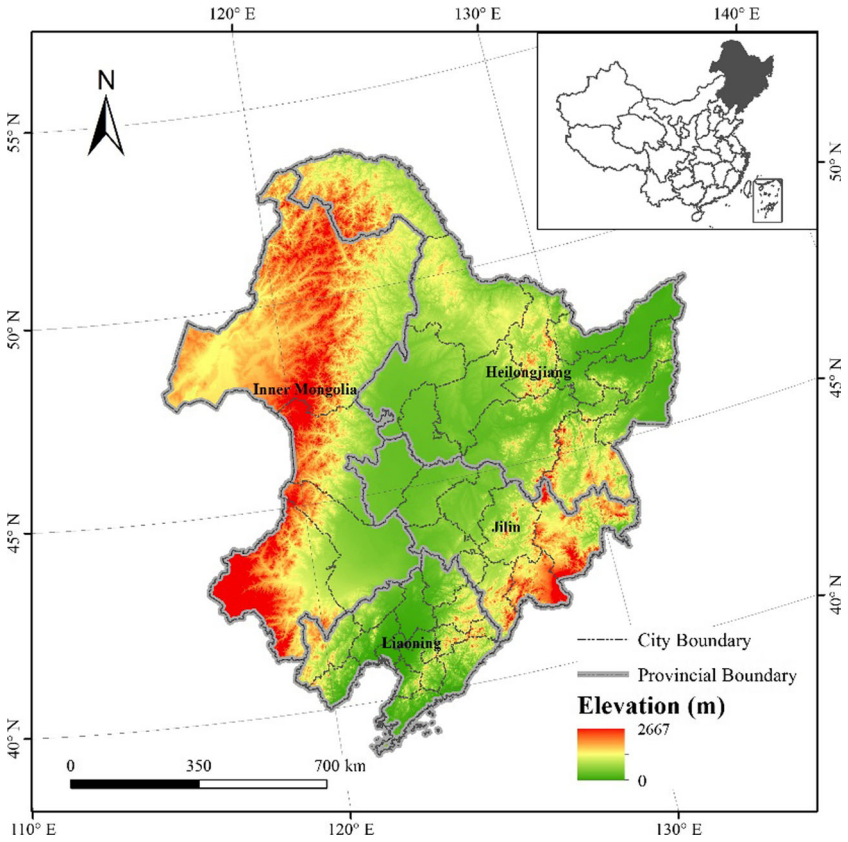

Fig. 1 Location of Northeast China

temperate zone, and forest steppe chernozem and meadow steppe chernozem in the temperate zone (Sun et al. 2006). Northeast China is mainly occupied by forest and farmland, which cover 39.87% and 33.77% of the total area respectively. Rice and maize are popular in Northeast China. The actual rice and maize production account for about 90% of the total grain production (including cereal, tuber, and soybean) in Northeast China in 2015 by referring to the Statistical Yearbook of Northeast China (Table 1).

2.2 Data sources

Climate, soil, terrain, farmland, and irrigation datasets were used in the GAEZ model. The data sources are detailed below. Besides, the agricultural statistical data on crop production were also needed.

2.2.1 Contemporary climate data

Seven kinds of climate variables were considered in this study to estimate the climate changes, including monthly mean maximum and minimum temperature, cumulative precipitation, cumulative net solar radiation, mean relative humidity, mean wind speed at 2 m height, and wet day frequency (the number of days on which the precipitation exceeds 0.2 mm). The wet day frequency variable data were needed from 1996 to 2015, while the other six variables data were needed in 2015. The contemporary climate data were obtained from the National Meteorological Information Center (http://www.nmic.cn/).

Table 1 Actual maize and rice production and total grain production in Northeast China in 2015

Province	Actual maize and rice production (million tonnes)	Total grain production (million tonnes)	Rate (%)
Heilongjiang	57.44	63.24	90.83
Jilin	34.35	36.47	94.19
Liaoning	18.71	20.02	93.45
Eastern parts of Inner Mongolia	20.25	22.62	89.52
Northeast China	130.75	142.35	91.85

The "Rate (%)" is the rate of actual maize and rice production to total grain production

These observations were from 99 meteorological stations distributed throughout Northeast China at a wide range of elevations. The above seven kinds of variables related to crop growth were all interpolated to 10 km spatial resolution raster data by using the ANUSPLIN software based on the DEM of Northeast China (Hutchinson 1995, 1998a, 1998b).

2.2.2 Future climate data

The future climate data were also needed in this study, including the seven climate variables above in 2050. Except wet day frequency, other six climate variables were derived from two RCP scenarios, RCP 4.5 and 6.0 in the IPCC's Fifth Assessment Report (AR5). Twelve climate models containing both emission scenarios were used to simulate future climate scenarios in this study, the details of which are shown in Table 2. The variables in the 12 climate models were all monthly average data in 2050, including "hurs" (near-surface relative humidity), "pr" (precipitation), "rsus" (surface upwelling shortwave radiation), "rsds" (surface downwelling shortwave radiation), "sfcWind" (near-surface wind speed), "tasmax" (maximum near-surface air temperature), and "tasmin" (minimum near-surface air temperature). The net solar radiation can be calculated by using "rsds" to minus "rsus."

The initial future climate data, NetCDF files, were transferred to raster data by using Python and Matlab. Due to the different and low spatial resolutions of the raster data from the 12 climate models, the climate model outputs of six variables were re-gridded to a resolution of 10 km × 10 km. The downscaling method was to transfer the raster data to points, and then use the ANUSPLIN software to interpolate to 10-km grid-cell surfaces based on the latitude, longitude, and elevation of each point. We first analyzed the characteristics of climate predicted results of 12 climate models in 2050 under RCP 4.5 and 6.0. Then, to reduce the errors of different predicted results as much as possible, the simple average method was applied for multi-model ensemble to obtain the monthly average data under RCP4.5 and 6.0 respectively. By comparing the climate predicted results with the climate conditions in 2015, the annual mean climate change maps of six climate variables during 2015–2050 were obtained.

As wet day frequency was not simulated in the future climate scenarios, we explored the interannual trend of wet day frequency in the last 20 years (1996–2015) (Fig. 2). We selected seven representative stations out of 99 meteorological stations in Northeast China, namely Mohe in the north (N) area, Harlaer in the northwest (NW) area, Chifeng in the southwest (SW) area, Anshan in the south (S) area, Tonghua in the southeast (SE) area, Jiamusi in the northeast (NE) area, and Baicheng in the central (C) area. As the growing seasons of maize and paddy rice extend from May to September in Northeast China, we analyzed the changes of wet day frequency from May to September in the last 20 years (Zhang and Huang 2012) (Fig. 2). It can be found that wet day frequency of seven meteorological stations has varied in the last 20 years, but has largely fluctuated on the horizontal lines no matter what month it is. Therefore, we used the wet day frequency in 2015 as the predicted wet day frequency in 2050.

2.2.3 Soil data

The soil data of Northeast China were extracted from the corresponding grid cell in the 1 km × 1 km Harmonized World Soil Database (HWSD) including various soil attributes such as soil texture, organic carbon content, soil acidity, soil drainage ability, and so on, which were developed by the International Institute for Applied Systems Analysis (IIASA) and Food and Agriculture Organization (FAO) (Yuji et al. 2009). The soil data also need to be processed to 10 km resolution grid.

Table 2 Summary of 12 global climate models from CMIP5 used in this study

No.	Climate Model	Country	Spatial resolution (grids, lon × lat)
1	GFDL-CM3	USA	144 × 90
2	GFDL-ESM2G	USA	144 × 90
3	GFDL-ESM2M	USA	144 × 90
4	HadGEM2-ES	UK	192 × 145
5	IPSL-CM5A-LR	France	96 × 96
6	IPSL-CM5A-MR	France	144 × 143
7	MIROC5	Japan	256 × 128
8	MIROC-ESM	Japan	128 × 64
9	MIROC-ESM-CHEM	Japan	128 × 64
10	MRI-CGCM3	Japan	320 × 160
11	GISS-E2-H	USA	144 × 90
12	GISS-E2-R	USA	144 × 90

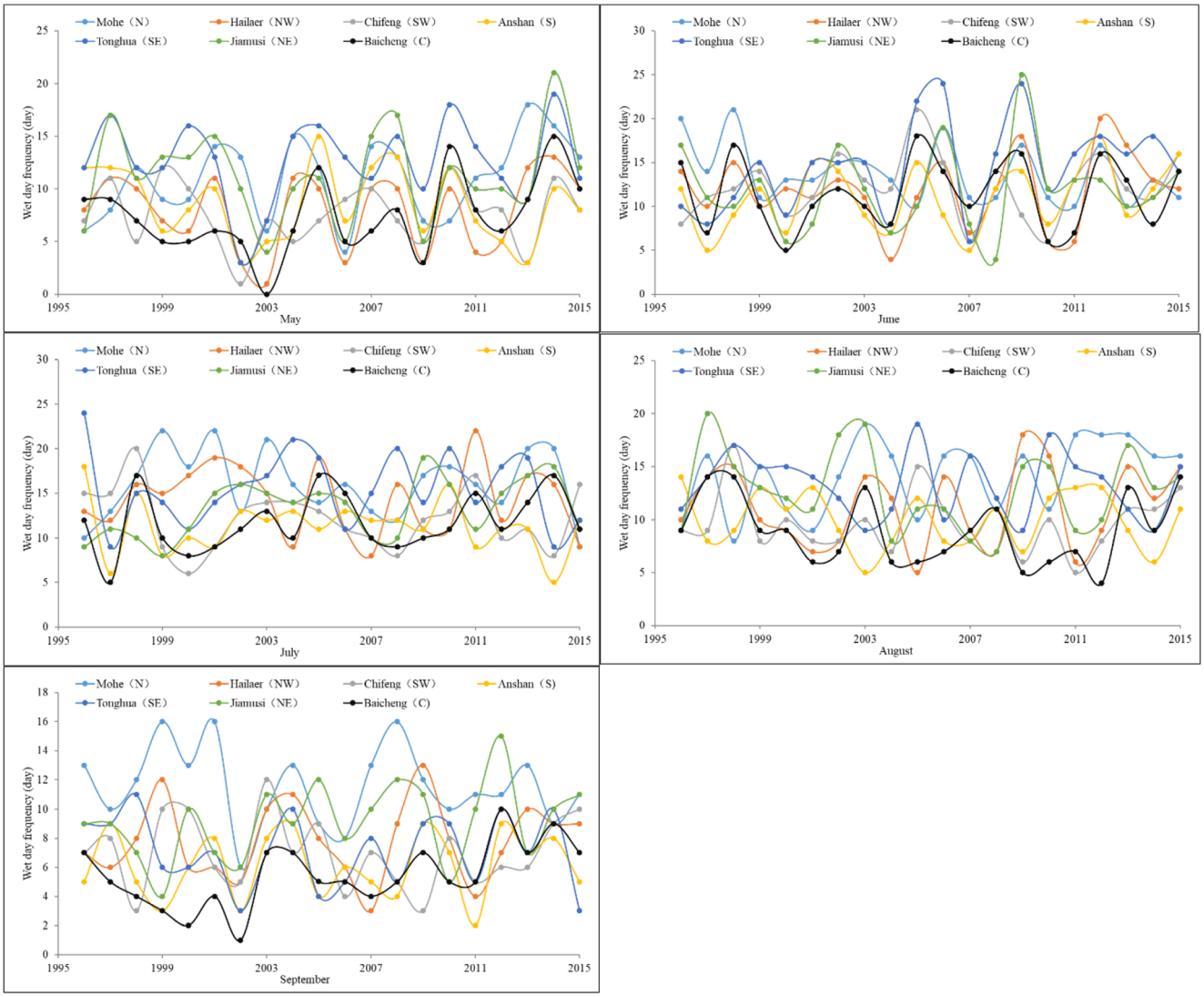

Fig. 2 Wet day frequency at 7 representative meteorological stations from May to September in the last 20 years

2.2.4 Terrain data

The terrain data, high-resolution raster DEM with 90 m spatial resolution, were from the Shuttle Radar Topography Mission (SRTM) C-band data (Shortridge and Messina 2011). The DEM data were processed into slope and aspect data and resampled to 10 km spatial resolution grid.

2.2.5 Farmland data

The farmland data in this study were extracted from the land use database of 2015 developed by the Chinese Academy of Sciences (with a mapping scale of 100,000) (http://www.resdc.cn/). The land use database was obtained from manual visual interpretation at Landsat Operational Land Imager (OLI) images in 2015. Through field verification, the interpretation precision was more than 90%, which could satisfy the accuracy requirement of 1:100,000 mapping (Liu et al. 2002, 2005). The land use data were divided into six major categories, including farmland, woodland, grassland, water bodies, built-up land, and unused land. The farmland was also divided into dryland and paddy field. Generally, maize was planted in dryland and rice in paddy field. As the input of farmland data in the GAEZ model is the last step and the resolution is arbitrary, the farmland data need to be processed to dryland and paddy field ratio data with 1 km spatial resolution grid in this study.

2.2.6 Irrigation data

The irrigation data in 2015 were the irrigation area ratio data of each city in Northeast China from the Statistical Yearbook of Northeast China. The irrigation data also need to be processed to 1 km spatial resolution grid in this study.

2.2.7 Agricultural statistical data on crop production

The agricultural statistical data on actual crop production of 2015 (Table 1) were also needed, deriving from the Statistical Yearbooks of Heilongjiang, Jilin, Liaoning, and Inner Mongolia in 2015.

2.3 Methods

2.3.1 Simulation of the GAEZ model

The GAEZ model was used to simulate the crop potential yield in this study, and was developed by the Food and Agricultural Organization (FAO) of the United Nations and the International Institute for Applied System (IIASA) (Fischer et al. 2002, 2008). The GAEZ model calculates crop productivity potential based on photosynthetic potential, light and temperature potential, climate production potential, and land production potential step by step (Liu et al. 2018). It employs simple and robust crop models and provides standardized crop-modeling and environmental matching procedure to identify crop-specific limitations of prevailing climate, soil and terrain resources under assumed levels of input and management conditions (Pu et al. 2018). In this study, the GAEZ model simulated the rice and maize potential yields in 2015 and 2050. Pu et al. have given a detailed description of the calculation procedures and validation of the GAEZ model (Pu et al. 2019).

So how do climate factors impact crop growth? In the GAEZ model, seven kinds of monthly mean climate variables impacting crop potential yields include relative humidity (RH), cumulative precipitation (P), mean maximum and minimum temperature (Tmax and Tmin), net solar radiation (SRn), wind speed (WS), and wet day frequency (WDF). Evapotranspiration was an important factor for crops to obtain biomass and yield. GAEZ model calculates reference evapotranspiration (ET_0) according to the Penman-Monteith equation firstly (Monteith 1981; Smith 1992). The WS, RH, SRn, Tmax, and Tmin were used for the estimation of ET_0. Then, the maximum evapotranspiration (ET_m) and actual evapotranspiration (Et_a) were calculated according to specific attributes of each crop and daily precipitation. WDF was used to derive daily precipitation events from monthly totals (P). Meantime, Tmin, Tmax, and P were also major determinants of crop growth and development. In GAEZ, the effects of temperature and precipitation were characterized in each grid-cell by thermal regimes, including thermal climates, thermal zones, length of temperature growing periods, temperature sums, and temperature profiles (Fischer et al. 2012).

2.3.2 Impact of future climate changes on the potential yields of maize and paddy rice

After simulating the potential yields of maize and paddy rice in 2050 under RCP 4.5 and 6.0, and the potential yields in 2015 using the GAEZ model, the temporal and spatial changes of maize and rice potential yields during 2015–2050 were obtained. Except climate variables, the other factors, including soil, terrain, farmland, irrigation and input and management level, should be unchanged in this study, so that ensuring crop potential yield changes were only affected by climate changes. Due to the lack of wet day frequency simulation in future climate models, the wet day frequency also remained unchanged from 2015 to 2050 in this study. To explore the impact of climate changes from 2015 to 2050 on maize and rice potential yields, the correlation matrixes were established and the correlation coefficients illustrated the correlativity between crop potential yield changes and climate changes.

3 Results

3.1 Characterization of future climate changes during 2015–2050 as projected by assemble of climate models

3.1.1 Climate prediction of 12 climate models in 2050 under RCP 4.5 and 6.0

To explore the characteristics of future climate predicted results of 12 climate models in 2050 under RCP 4.5 and 6.0, six annual mean climate variables of 12 climate models in 2050 were calculated including mean relative humidity (RH), cumulative precipitation (P), mean surface wind speed (WS), mean maximum temperature (Tmax), mean minimum temperature (Tmin), and cumulative net solar radiation (SRn), and were presented in the box plots (Fig. 3). It can be clearly seen that the predicted results of 12 climate models were very different regardless of the climate variables and RCP scenarios. The annual RH were 64.84–83.40% under RCP 4.5 and 64.19–84.33% under RCP 6.0 in 12 climate models, and the values under RCP 6.0 were more aggregate than that under RCP 4.5. As for the annual P, although the value range under RCP 4.5 was larger than that under RCP 6.0, it was much more aggregate than that under RCP 6.0. The value range of the annual WS under RCP 4.5 was a little larger than that under RCP 6.0, and the values were a little more diffuse than that under RCP 6.0. The value ranges of the annual Tmax were close between RCP 4.5 and 6.0, but the values were more aggregate under RCP 4.5. The biggest annual Tmin under RCP 4.5 in 12 climate models was 1.82 °C, which was much higher than 0.33 °C under RCP 6.0. The smallest Tmin were close under two RCPs. The annual SRn were 3574.28–4599.71 MJ/m^2/a under RCP 4.5 and 3695.91–4485.87 MJ/m^2/a under RCP 6.0, and the values were more diffuse under RCP 4.5. In short, 12 climate models predicted different results of six climate variables. It was difficult to determine which predicted result was the most accurate

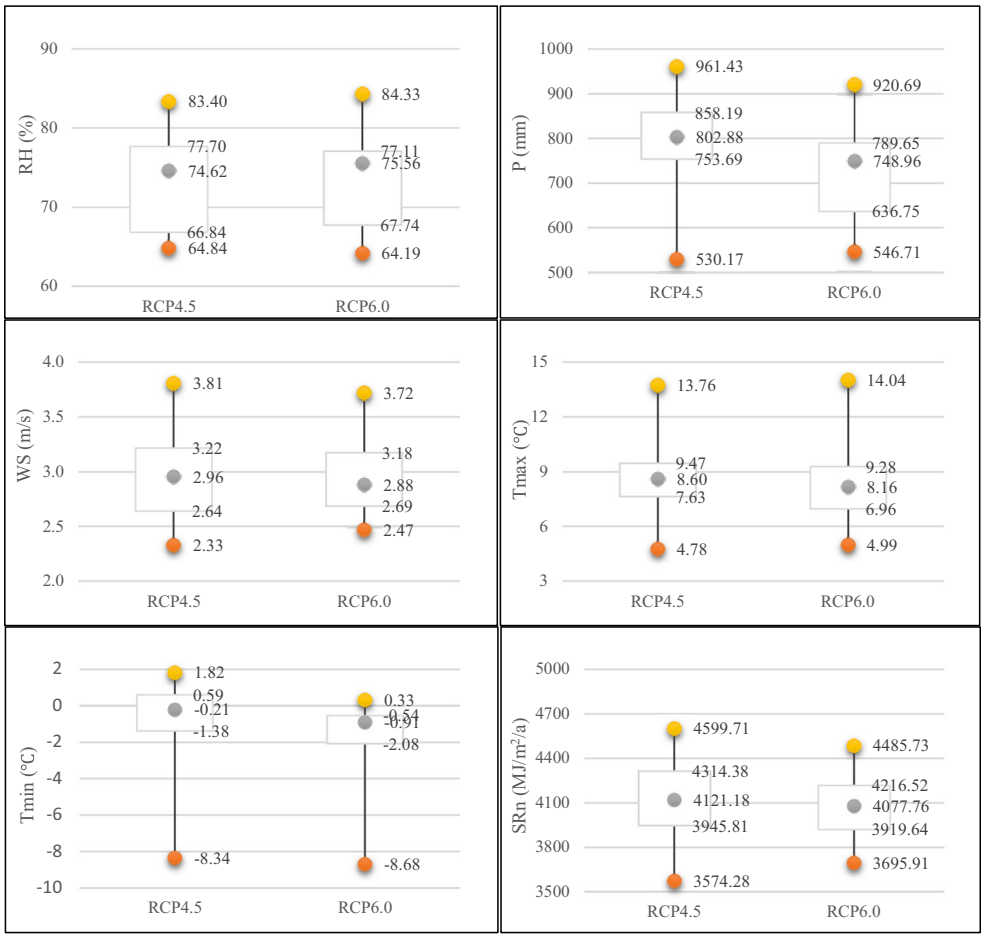

Fig. 3 Comparison of six climate variables of 12 climate models in 2050 under RCP 4.5 and 6.0

among 12 climate models, so the multi-model ensemble was used to reduce the errors of different predicted results as much as possible. We averaged simply the predicted results of 12 climate models and used the results as climate conditions in 2050.

3.1.2 Climate changes from 2015 to 2050 under RCP 4.5 and 6.0

After obtaining the average predicted results of the six climate variables of 12 climate models, the climate change characteristics from 2015 to 2050 are shown in Fig. 4. The climate changed a lot from 2015 to 2050. The change trends of the same variables were almost consistent under RCP 4.5 and 6.0 (Fig. 4a–l). From Fig. 4a and b, it can be seen that the changes of RH were similar under two RCPs. It increased almost throughout the Northeast China from 2015 to 2050, and the RH in the western region increased more than that in the eastern region. As for the annual P, it increased more under RCP 4.5 than that under RCP 6.0 from 2015 to 2050 (Fig. 4c, d). Spatially, the P increased in most areas of Northeast China under RCP 4.5, and decreased slightly in some areas under RCP 6.0. Besides, the P increased more than 400 mm in some west, east, and south regions under RCP 4.5. The change of annual WS was almost the same under two RCPs (Fig. 4e, f). It was obvious that the changes of WS were related to longitude closely, which increased gradually from east to west (Fig. 4g, h). In the west region, it even increased over 2 m/s. Figure 4g and h showed the changes of annual Tmax. We can see that the Tmax increased more under RCP 4.5 than that under RCP 6.0. In the west and north regions, the Tmax decreased, but increased in the other regions. Even in the northeast and southeast regions, the Tmax increased more than 2 °C. The annual Tmin increased much more under RCP 4.5 than that under RCP 6.0 (Fig. 4i, j). Under RCP 4.5, it almost increased in the whole region, but decreased in most center and northeast regions under RCP 6.0. It was also of interest that the changes of Tmax and Tmin were closely related to the terrain. We can see that the Tmax and Tmin increased more in the higher areas, and increased less or even decreased in the flat plain areas. As for the annual SRn, it varied significantly with latitude (Fig. 4k, l). The lower the latitude, the more the SRn increased. In the south region, the SRn increased more than 1200 MJ/m^2/a under two RCPs.

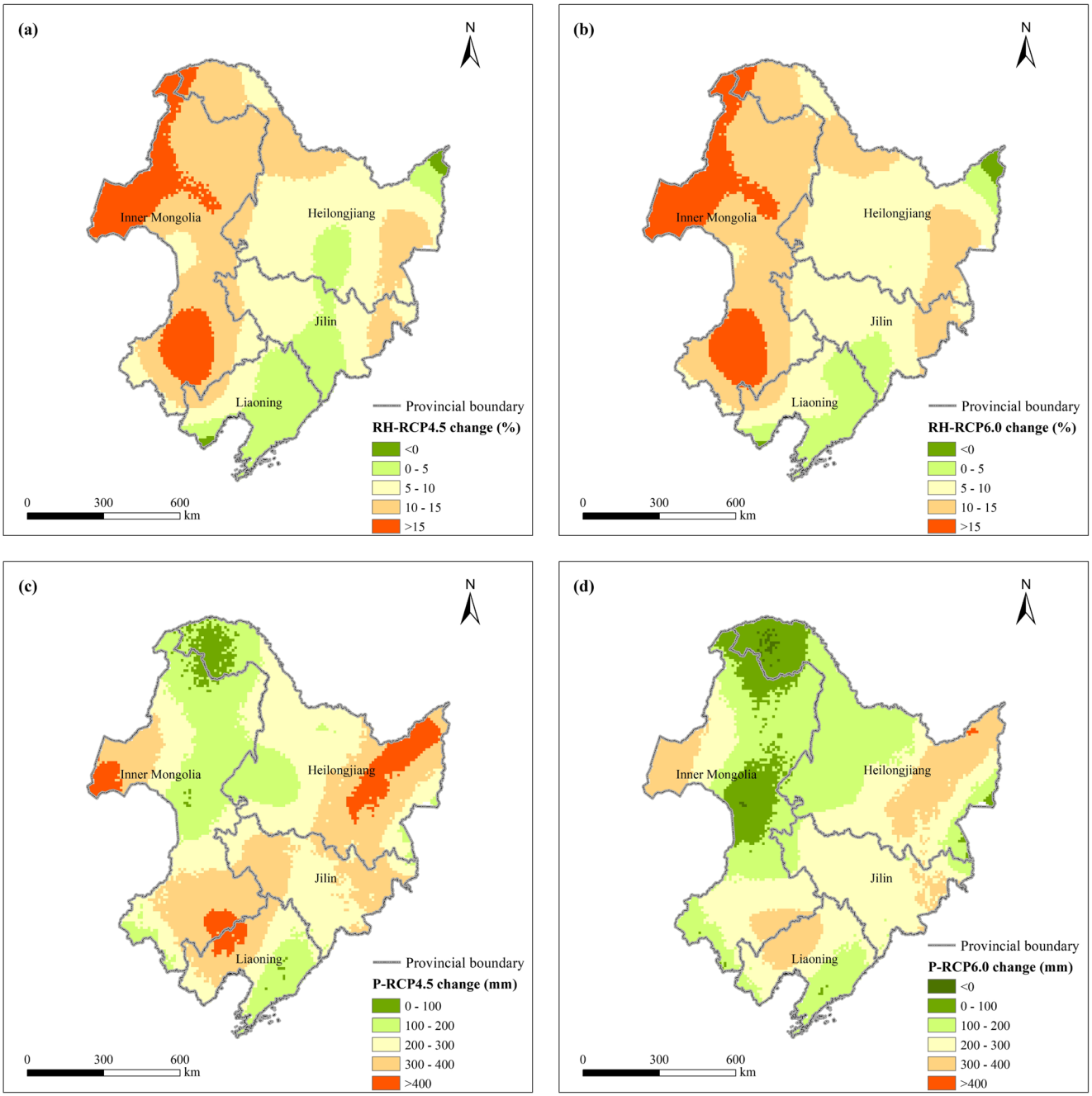

Fig. 4 Changes of six climate variables from 2015 to 2050 under RCP 4.5 and 6.0. **a** RH-RCP4.5 change. **b** RH-RCP6.0 change. **c** P-RCP4.5 change. **d** P-RCP6.0 change. **e** WS-RCP4.5. **f** WS-RCP6.0. **g** Tmax-RCP4.5. **h** Tmax-RCP6.0 change. **i** Tmin-RCP4.5 change. **j** Tmin-RCP6.0 change. **k** SRn-RCP4.5 change. **l** SRn-RCP6.0 change

3.2 Maize and rice potential yields in 2050 and yield changes during 2015–2050

3.2.1 Maize potential yields in 2050 and yield changes under two RCPs

Using the GAEZ model, this study simulated the maize potential yields in Northeast China in 2015 and 2050 based on the climate data in 2015, climate projection results in 2050, soil data, DEM data, farmland and irrigation data of 2015 under two RCPs, and then calculated the maize potential yield changes during 2015–2050 (Figs. 5 and 6). The total maize potential production in Northeast China in 2050 under RCP 4.5 was 324.26 million tonnes (Fig. 5a). As the crop production is equal to yield times crop planting area, and the dryland area was 35.60 million ha, the average maize potential yield was 9108.87 kg/ha. In Fig. 5a the potential yield in the center region was much higher than that in the other regions. The potential yield in the center region was

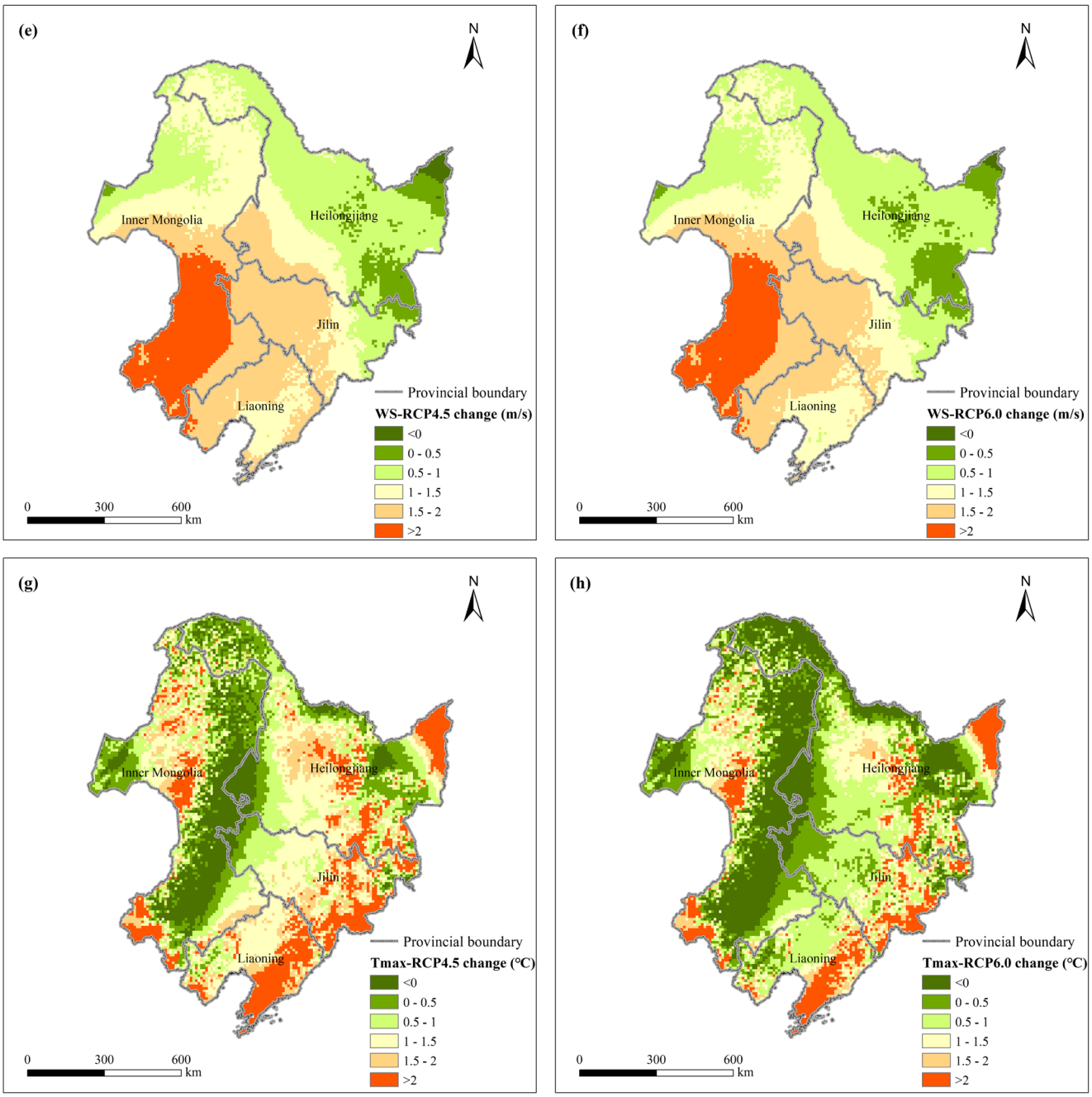

Fig. 4 continued.

more than 6000 kg/ha, and even exceeded 10,000 kg/ha in some center areas. In the other regions, such as the west, east, and south regions, the yield was less than 4000 kg/ha. Figure 5b showed the maize potential yield change during 2015–2050 under RCP 4.5. The maize potential production increased by 82.84 million tonnes from 2015 to 2050, and the average potential yield increased by 34.31% (2327.10 kg/ha) (Fig. 5b). Therefore, the total maize potential production and yield increased with the impact of climate changes during 2015–2050. Spatially, the maize potential yield increased almost in the whole region, which increased by more than 1500 kg/ha especially in the center and northwest areas. The potential yield increased by 1000–1500 kg/ha in the northeast area, and less than 1000 kg/ha in the southeast area.

Under RCP 6.0, the total maize potential production in 2050 was 303.30 million tonnes and the average potential yield was 8520.04 kg/ha, which were all less than that under RCP 4.5 (Fig. 6a). The spatial distribution of maize potential yield under RCP 6.0 was similar with that under RCP 4.5. The potential yield in the center region was much higher than that in the other regions. The yield in the center region was more than 6000 kg/

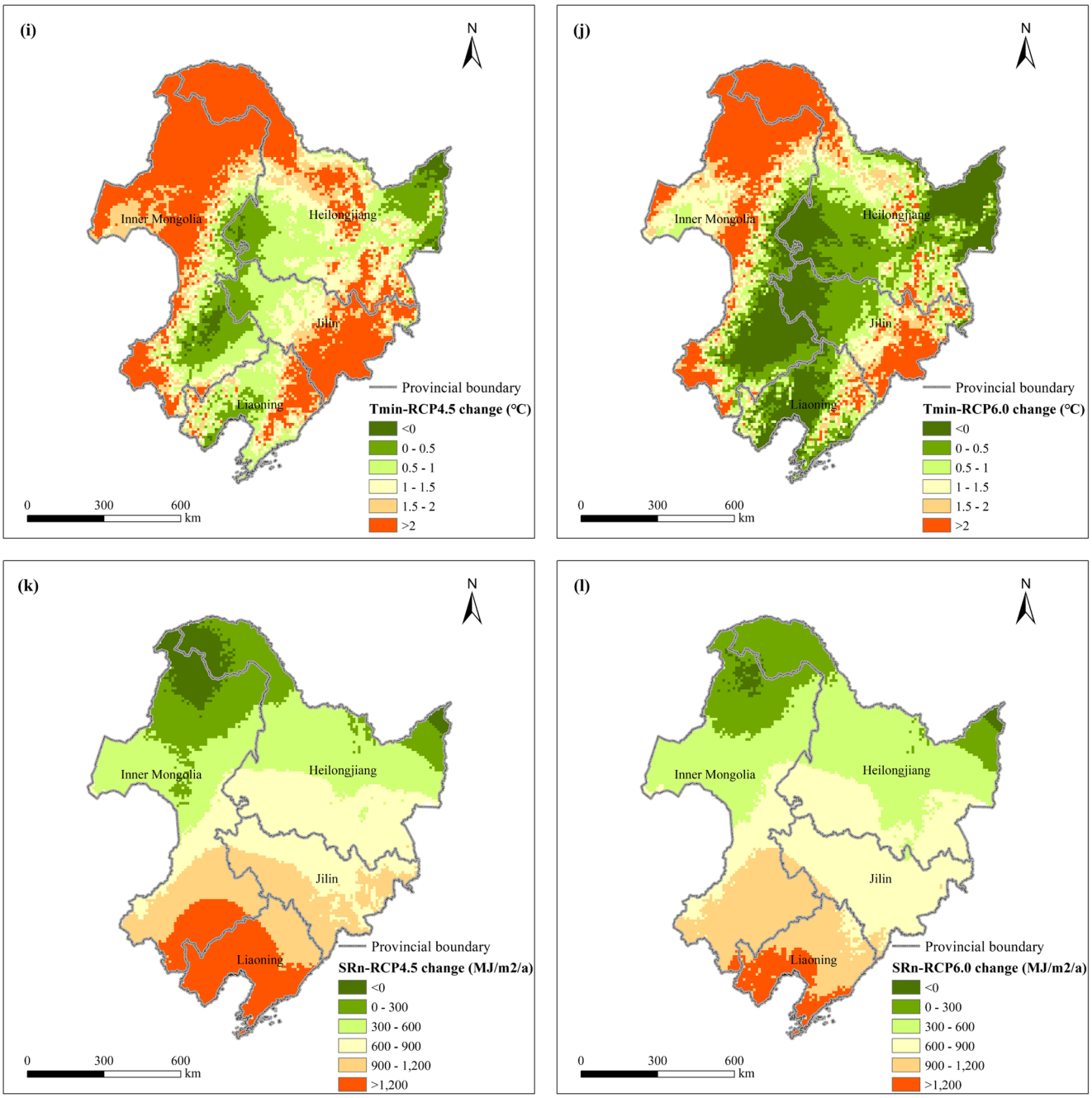

Fig. 4 continued.

ha, and in the other regions, such as the west, east, and south regions, the yield was less than 4000 kg/ha. The total maize potential production increased by 61.88 million tonnes from 2015 to 2050, and the average maize potential yield increased by 1739.27 kg/ha (25.65%) (Fig. 6b). As for the spatial distribution of maize potential yield change from 2015 to 2050, it can be seen that in the north area, it decreased during 2015–2050. In the center and northwest areas, it increased by more than 1000 kg/ha, and even more than 1500 kg/ha in the southwest area. In the other areas, the maize potential yield grew up by less than 1000 kg/ha.

3.2.2 Paddy rice potential yields in 2050 and yield changes under two RCPs

In paddy field, the total rice potential production in Northeast China in 2050 under RCP 4.5 was 39.84 million tonnes (Fig. 7a). The paddy field area was 6.36 million ha, so the average rice potential yield was 6264.08 kg/ha. The potential yield in the northeast region, where the Sanjiang Plain was located, was more than 6000 kg/ha, much higher than that in the other regions. In the other regions, such as the west, east, and south regions, the yield was less than 4000 kg/ha. Under the impact of climate

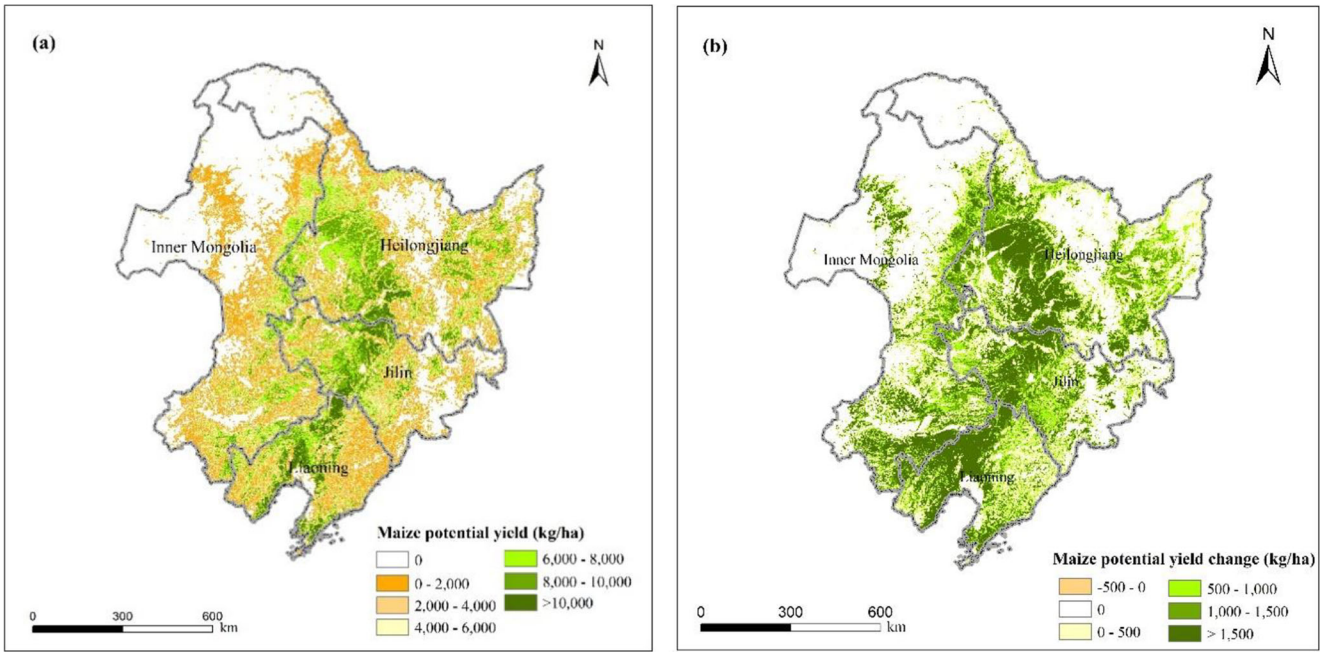

Fig. 5 Maize potential yield in 2050 and yield change from 2015 to 2050 under RCP 4.5. **a** Maize potential yield. **b** Maize potential yield change

changes, the rice potential production and yield increased under RCP 4.5 (Fig. 7b). The total rice potential production increased by 5.73 million tonnes during 2015–2050 under RCP 4.5, and the average potential yield increased by 901.88 kg/ha (16.82%). In most areas, the rice potential yield increased, and even increased by more than 500 kg/ha in the northeast area. In the center area of Heilongjiang Province, it grew up by more than 1000 kg/ha.

The total rice potential production in 2050 under RCP 6.0 was 36.28 million tonnes, and the average rice potential yield was 5703.45 kg/ha (Fig. 8a). The rice potential production and yield under RCP 6.0 were also less than that under RCP 4.5. The potential yield in the place where the Sanjiang Plain was located was also more than 6000 kg/ha. In the other regions, such as the west, east, and south regions, the yield was less than 4000 kg/ha. The rice potential production increased by 2.17 million tonnes under RCP 6.0 from 2015 to 2050, and the average potential yield increased by 340.25 kg/ha (6.34%) (Fig. 8b). In most areas, the rice potential yield increased by less than 500 kg/ha, but in the northeast area, it decreased.

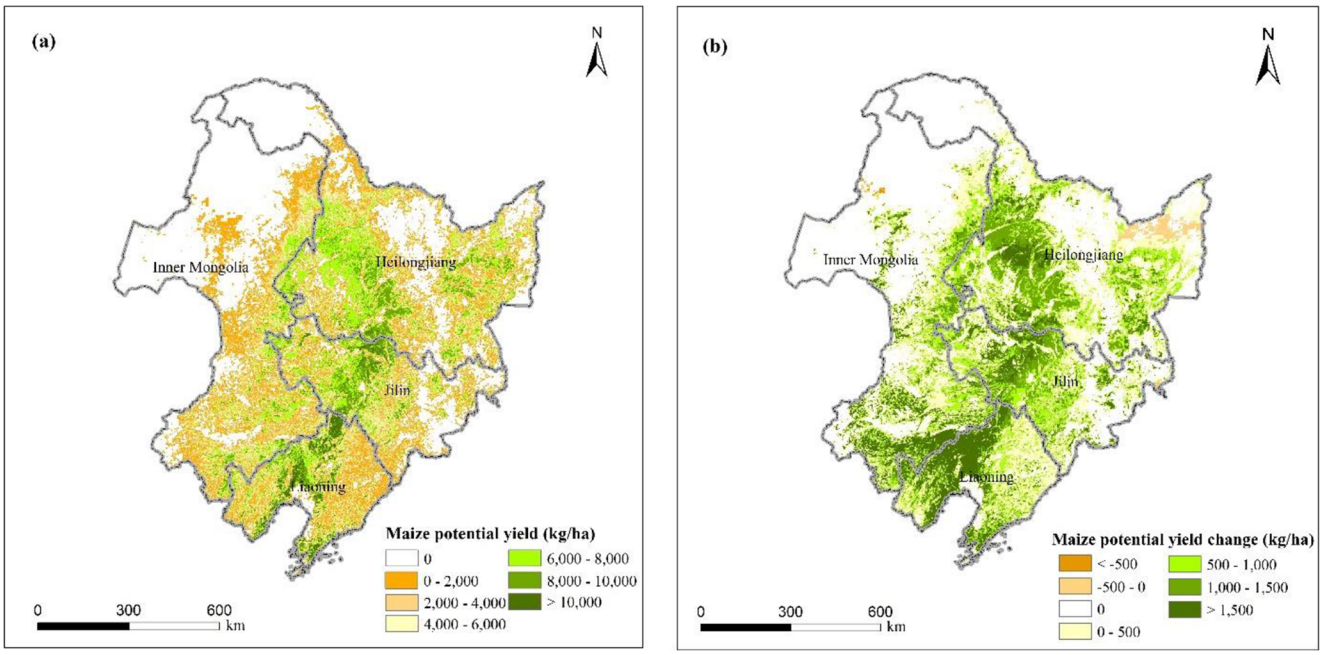

Fig. 6 Maize potential yield in 2050 and yield change from 2015 to 2050 under RCP 6.0. **a** Maize potential yield. **b** Maize potential yield change

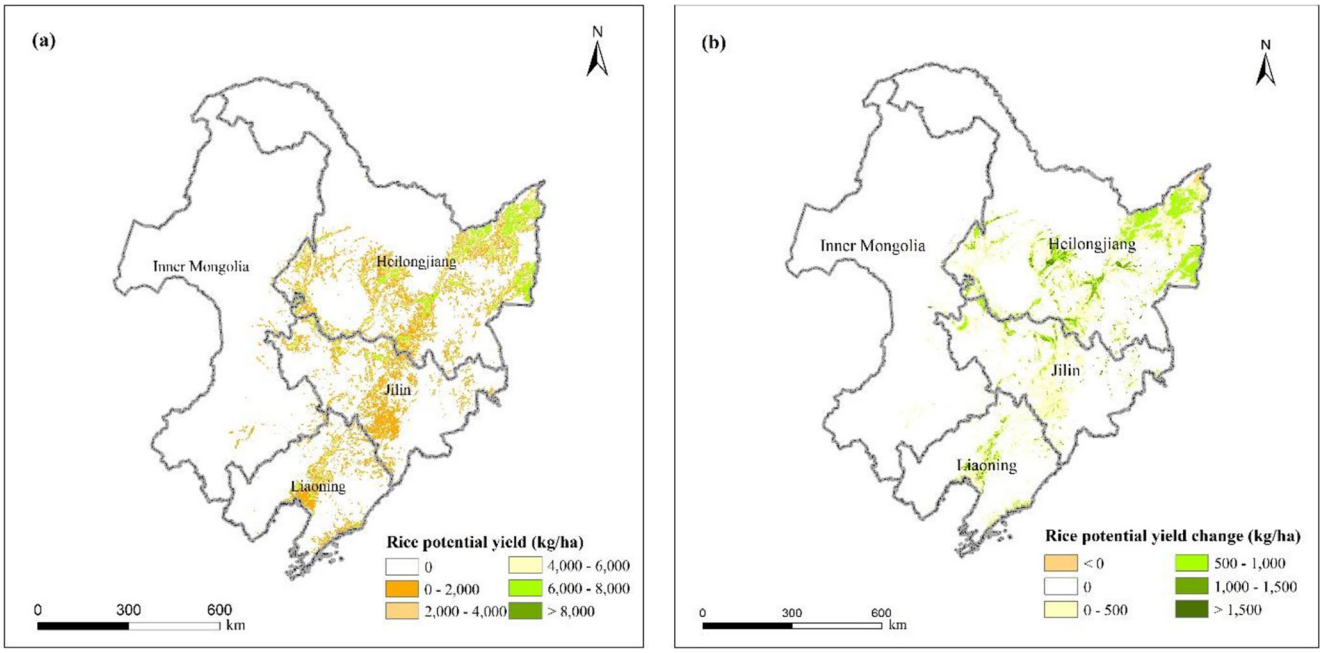

Fig. 7 Paddy rice potential yield in 2050 and yield change from 2015 to 2050 under RCP 4.5. **a** Rice potential yield. **b** Rice potential yield change

3.3 Impacts of future climate changes on maize and paddy rice yields

Two correlation matrixes were established to analyze the impact of climate changes on maize and rice potential yields during 2015–2050 using the "Band Collection Statistics" tool in ArcGIS, and the correlation coefficients in the forms showed the correlativity between maize and rice potential yield changes and climate changes under two RCPs (Tables 3 and 4). The absolute value of the correlation coefficient is approximately 1, indicating that the correlation between the two layers is stronger. When the correlation coefficient is greater than 0, the two layers are positively correlated and vice versa. In the two forms, ΔY_m and ΔY_r represented the maize and rice potential yield changes, and ΔRH, ΔP, ΔWS, ΔTmax, ΔTmin, and ΔSRn were the changes of RH, P, WS, Tmax, Tmin, and SRn from 2015 to 2050 respectively. From Table 3, ΔY_m was positively correlated with ΔP (0.21), ΔWS (0.25), and ΔSRn (0.40), meaning that increasing precipitation, wind speed, or net solar radiation was good

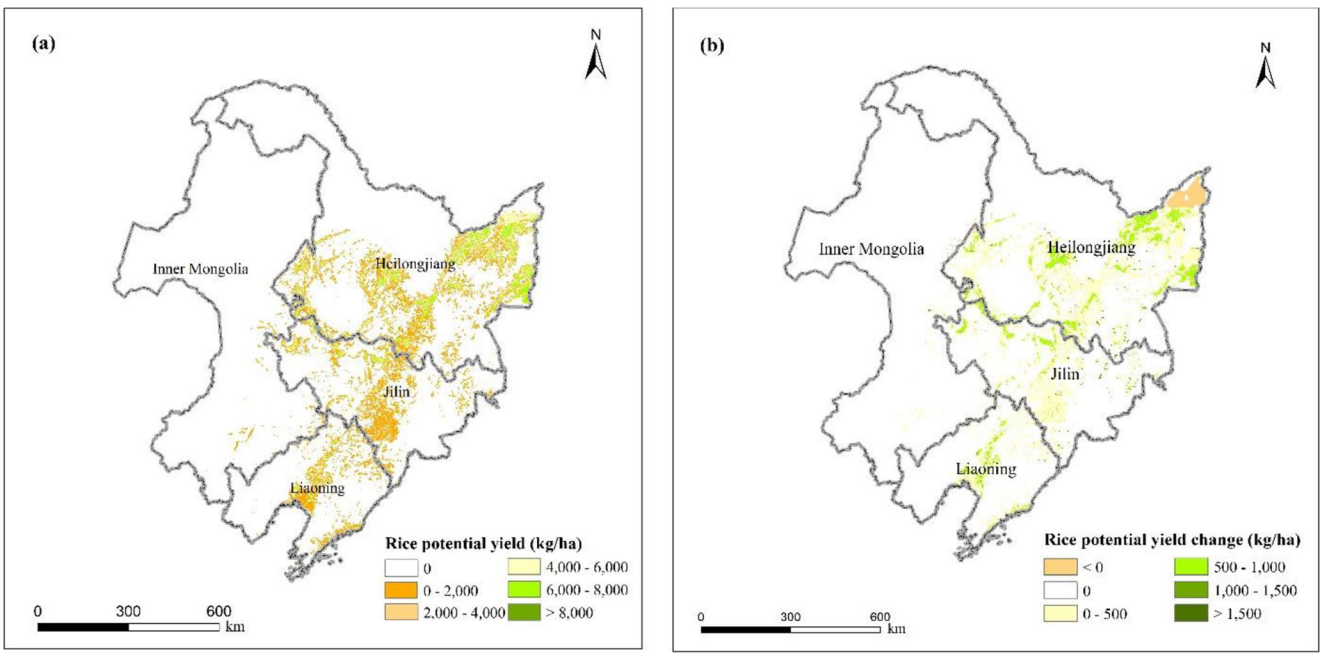

Fig. 8 Paddy rice potential yield in 2050 and yield change from 2015 to 2050 under RCP 6.0. **a** Rice potential yield. **b** Rice potential yield change

Table 3 Correlation matrix under RCP 4.5

	ΔY_m	ΔY_r	ΔRH	ΔP	ΔWS	ΔTmax	ΔTmin	ΔSRn
ΔY_m	1.00	–	− 0.16	0.21	0.25	− 0.02	−0.34	0.40
ΔY_r		1.00	− 0.18	0.15	− 0.12	0.02	−0.19	0.00
ΔRH			1.00	− 0.03	0.10	− 0.54	0.22	− 0.36
ΔP				1.00	− 0.05	0.00	−0.53	0.38
ΔWS					1.00	− 0.32	−0.26	0.57
ΔTmax						1.00	0.28	0.11
ΔTmin							1.00	− 0.52
ΔSRn								1.00

for maize growth under RCP 4.5. The maximum correlation coefficient between ΔY_m and ΔSRn was 0.40, indicating that the increase of net solar radiation contributed the most to the growth of maize potential yield. ΔY_m was negatively correlated with ΔRH (− 0.16), ΔTmax (− 0.02), and ΔTmin (− 0.34), but the correlation coefficients between ΔY_m and ΔTmax were close to 0, meaning that the increase of mean maximum temperature had little impact on maize potential yield under RCP 4.5. The increase of Tmin will greatly reduce the maize potential yield. ΔY_r was positively correlated with the changes of ΔP (0.15), but almost not affected by the changes of mean maximum temperature and net solar radiation. The increase of RH, WS, and Tmin will reduce the rice potential yield. There was also a clear correlation between different climate variables. For example, there were strong negative correlations between ΔRH and ΔTmax (− 0.54), between ΔP and ΔTmin (− 0.53), and between ΔTmin and ΔSRn (− 0.52). However, ΔWS and ΔSRn had a strong positive correlation (0.57).

Under RCP 6.0, ΔY_m was positively correlated with ΔP (0.21), ΔWS (0.27), and ΔSRn (0.43), and negatively correlated with ΔRH (− 0.13), ΔTmax (− 0.03), and ΔTmin (− 0.32) under RCP 6.0 (Table 4). ΔY_m and ΔSRn had a strong positive correlation and the correlation coefficient was 0.43. ΔY_m and ΔTmin had a clear negative correlation and the coefficient was − 0.32. As for ΔY_r, it had a slight positive correlation with ΔSRn (0.10), ΔRH (0.06), and ΔWS (0.07), and slight negative correlation with ΔTmax (− 0.15). There were also strong negative correlations between ΔRH and ΔTmax (− 0.46), between ΔP and ΔTmin (− 0.48), and between ΔTmin and ΔSRn (− 0.53). ΔWS and ΔSRn had a strong positive correlation (0.62).

4 Discussions

4.1 Uncertainty of predicting future climate

A major uncertainty in this study is the prediction of future climate conditions resulted from different emission scenarios and climate models. Although in order to eliminate the errors of the predicted results in different climate models as much as possible, we selected the predicted results of 12 climate models containing both emission scenarios (RCPs) and used the simple average method, other climate scenarios are likely to give different characteristics of future climate. Therefore the uncertainty of future climate change is still a significant source of uncertainty in this paper (Alcamo et al. 2007).

The climate variable in 2050, wet day frequency, had to be assumed to remain unchanged from that in 2015 in this study since the wet day frequency variable was not simulated in the future climate model in CMIP5. Although it was verified in Part 2.3.1 that the wet day frequency fluctuated on the horizontal lines, replacing the predicted wet day frequency in

Table 4 Correlation matrix under RCP 6.0

	ΔY_m	ΔY_r	ΔRH	ΔP	ΔWS	ΔTmax	ΔTmin	ΔSRn
ΔY_m	1.00	–	− 0.13	0.21	0.27	− 0.03	− 0.32	0.43
ΔY_r		1.00	0.06	− 0.01	0.07	− 0.15	− 0.01	0.10
ΔRH			1.00	− 0.20	0.16	− 0.46	0.29	− 0.24
ΔP				1.00	− 0.11	0.10	− 0.48	0.32
ΔWS					1.00	− 0.28	− 0.27	0.62
ΔTmax						1.00	0.29	0.03
ΔTmin							1.00	− 0.53
ΔSRn								1.00

2050 with that in 2015 may cause the errors in daily precipitation, because the wet day frequency was used to divide the total monthly precipitation into daily rainfall, thus leading to errors in crop potential yields. Therefore, future study will need to focus on finding better algorithms to estimate the future wet day frequency, so simulation of future crop potential yield will be more accurate.

4.2 Uncertainty of the GAEZ model

Actually, the GAEZ model used in this study has some limitations. First, because the spatial resolution of initial future climate data in the GCMs was rough and spatial resolution of climate data input to the GAEZ model should be 10 km × 10 km, the initial future climate data were downscaled and interpolated using the Anusplin software. Although compared with other interpolation methods, the surfaces obtained by the Anusplin method were more realistic, it was still hard to obtain completely accurate spatial distribution maps. This increased the uncertainty of future climate conditions in small regions, and further increased the uncertainty of crop potential yield in small regions. It would be a long way to explore more ideal interpolation method to reduce the results errors as much as possible.

Second, as future climate scenarios cannot predict extreme climate conditions and the input climate data to the GAEZ model should be monthly average data, the GAEZ model has not been able to simulate crop potential yield under extreme weather. Extreme weather, especially extreme temperature and precipitation, may have large effects on crop growth.

Third, this study used only one crop model (GAEZ) to simulate crop potential yields. The parameters of the particular crop type or the process of calculating crop yield may vary in different models, which may cause small differences. Some scholars reported that ensembles of many models could give a better estimate of crop yields than using only one model (Asseng 2013; Martre et al. 2015). Multi-crop model and multi-GCM ensemble projections are recommended for studies of impact of climate changes on crop yields (Araya et al. 2015).

4.3 Advantage of impact of future climate changes on crop potential yields analysis method

In general, crop potential yield was largely affected by various variables, including climate variables, soil quality, terrain, irrigation condition, farmland area and distribution, and human input and management. However, the objective of this study is to analyze the impact of future climate changes on crop potential yields. Therefore, to prevent the other factors except climate variables from affecting crop yields, these factors had to remain unchanged during the study period. This is called "control variate method." By using this method, the results in this study could directly show the impact of future climate changes and were relatively accurate.

5 Conclusions

In this study, six future climate variables in 2050 under RCP 4.5 and 6.0 were simulated using 12 climate models in CMIP5, and the predicted results were very different from 12 climate models. Hence, the multi-model ensemble, a simple average of the predicted results of 12 climate models, was used to reduce the errors of different predicted results as much as possible. The change trends of the same variables were almost consistent under RCP 4.5 and 6.0 during 2015–2050. The annual RH increased almost throughout the Northeast China from 2015 to 2050, and increased in the western region more than that in the eastern region. The annual P increased more than 400 mm in some west, east, and south areas under RCP 4.5, but decreased slightly in some places under RCP 6.0. The annual WS change was related to longitude closely, which increased gradually from east to west. The annual SRn change varied significantly with latitude and increased gradually from north to south. The changes of annual Tmax and Tmin were closely related to the terrain.

The maize and rice total potential production and total average yields all showed an increasing trend under two RCPs with the impact of climate changes from 2015 to 2050. Under RCP 4.5, the total maize potential production in Northeast China in 2050 was 324.26 million, and the average potential yield was 9108.87 kg/ha. From 2015 to 2050, the maize potential production and average potential yield increased by 82.84 million tonnes and 2327.10 kg/ha (34.31%) respectively. The maize potential yield increased by more than 1500 kg/ha in the center and northwest areas, much more than that in the other areas. Under RCP 6.0, the total maize potential production in 2050 was 303.30 million tonnes, 61.88 million tonnes more than in 2015. The average potential yield was 8520.04 kg/ha in 2050, increasing by 20.41% from 2015 to 2050. The total rice potential production and average potential yield in 2050 were 39.84 million tonnes and 6264.08 kg/ha respectively under RCP 4.5. The rice potential production increased by 5.73 million tonnes during 2015–2050, and the average potential yield increased by 901.88 kg/ha (16.82%). Under RCP 6.0, the total rice potential production in 2050 was 36.28 million tonnes, and the average potential yield was 5703.45 kg/ha. The rice potential production increased by 2.17 million tonnes from 2015 to 2050, and the average potential yield increased by 6.34%.

Under two RCPs, ΔY_m was positively correlated with ΔP, ΔWS, and ΔSRn, meaning that increasing precipitation, wind speed, or net solar radiation would promote the maize growth, and negatively correlated with ΔRH, $\Delta Tmax$, and $\Delta Tmin$. ΔY_r was positively correlated with ΔP, but almost not

affected by ΔTmin and ΔSRn under RCP 4.5. Under RCP 6.0, ΔY_r had a slight positive correlation with ΔSRn, ΔRH, and ΔWS, and slight negative correlation with ΔTmax.

It is very significant to evaluate crop responses to future climate changes. Although current assessment system cannot avoid the uncertainty about future climate conditions and the accuracy of crop models, and the farmland, irrigation conditions, even the soil characteristics may change in 2050, our study still can provide a general indication and guidance of the impact of climate changes in Northeast China. The results are valuable for guiding adaption efforts, providing reference information for policy makers and ensuring food security in the future.

Acknowledgments We thank the Center for Spatial Analysis, University of Oklahoma (OU), USA. We also thank Xiaocui Wu, Jilin Yang, Wen Zhuo, and HaoranYang of OU for their help.

Funding information This work was funded by the auspices of Multi-source heterogeneous data acquisition technology and data integration (No. XDA2003020301), National Key Research and Development Program (No. 2017YFC0504202), Technological Basic Research Program of China (No. 2017FY101301) and China Scholarship Council (No. 201806170212).

References

Alcamo J, Dronin N, Endejan M, Golubev G, Kirilenko A (2007) A new assessment of climate change impacts on food production shortfalls and water availability in Russia. Glob Environ Chang 17(3–4):429–444

Araya A, Hoogenboom G, Luedeling E, Hadgu K, Kisekka I, Martorano L (2015) Assessment of maize growth and yield using crop models under present and future climate in southwestern Ethiopia. Agric For Meteorol 214-215:252–265

Araya A, Kisekka I, Lin X, Prasad P, Gowda P, Rice C, Andales A (2017) Evaluating the impact of future climate change on irrigated maize production in Kansas. Clim Risk Manag 17:139–154

Asseng S (2013) Uncertainty in simulating wheat yields under climate change. Nat Clim Chang 3(9):827–832

Bassu et al (2014) How do various maize crop models vary in their responses to climate change factors? Glob Chang Biol 20(7): 2301–2320

Cannon R (1998) The implications of predicted climate change for insect pests in the UK, with emphasis on nonindigenous species. Glob Chang Biol 4:785–796

Chen X, Chen F, Chen Y, Gao Q, Yang X, Yuan L, Zhang F, Mi G (2013) Modern maize hybrids in Northeast China exhibit increased yield potential and resource use *effi*ciency despite adverse climate change. Glob Chang Biol 19:923–936

Diepen C, Wolf J, Keulen H (2010) WOFOST: a simulation model of crop production. Soil Use Management 5:16–24

Fischer G, Shah M, Van Velthuizen H, Nachtergaele FO (2002) Global agro-ecological assessment for agriculture in the 21st century:methodology and results. IIASA RR-02-02, IIASA, Laxenburg, Austria

Fischer G, Nachtergaele S, Prieler H et al (2008) Global agro-ecological zones assessment for agriculture (GAEZ 2008). IIASA, Laxenburg, Austria and FAO, Rome

Fischer G, Nachtergaele FO, Prieler S, et al (2012) Global Agro-ecological Zones (GAEZ v3. 0)-Model Documentation

Gao G, Jie D, Wang Y, Liu L, Liu H, Li D, Li N, Shi J, Leng C (2018) Do soil phytoliths accurately represent plant communities in a temperate region? A case study of Northeast China. Veg Hist Archaeobotany:1–13

Hutchinson M (1995) Interpolating mean rainfall using thin plate smoothing splines. Int J Geogr Inf Syst 9:385–403

Hutchinson M (1998a) Interpolation of rainfall data with thin plate smoothing splines-Part I: Two dimensional smoothing of data with short range correlation. J Geogr Inf Decis Anal 2(2):139–151

Hutchinson M (1998b) Interpolation of rainfall data with thin plate smoothing splines-Part II: Analysis of topographic dependence. J Geogr Inf Decis Anal 2(2):152–167

Izaurralde R, Williams J, McGill W, Rosenberg N, Jakas M (2006) Simulating soil C dynamics with EPIC: model description and testing against long-term data. Ecol Model 192(3–4):362–384

Jones P, Thornton P (2003) The potential impacts of climate change on maize production in Africa and Latin America in 2055. Glob Environ Chang 13:51–59

Kassie BT, Asseng S, Rötter RP et al (2015) Exploring climate change impacts and adaptation options for maize production in the central rift valley of Ethiopia using different climate change scenarios and crop models. Clim Chang 129(1–2):145–158

Liu J, Liu M, Deng S et al (2002) The land use and land cover change database and its relative studies in China. J Geogr Sci 12(3):275–282

Liu J, Liu M, Tian H et al (2005) Spatial and temporal patterns of China's cropland during 1990-2000: an analysis based on Landsat TM data. Remote Sens Environ 98(4):442–456

Liu L, Xu X, Hu Y, Liu Z, Qiao Z (2018) Efficiency analysis of bioenergy potential on winter fallow fields: a case study of rape. Sci Total Environ 628-629:103–109

Lu X, Ren C, Wang Y, Cui F, Lu X, Gong Z (2018) Spatial difference characteristics on simulation capability of seasonal variation of air temperature simulated by three global climate models in China. Arid Land Geography 41(05):972–983

Lv S, Yang X, Lin X, Liu Z, Zhao J, Li K, Mu C, Chen X, Chen F, Mi G (2015) Yield gap simulations using ten maize cultivars commonly planted in Northeast China during the past five decades. Agric For Meteorol 205:1–10

Mao D, Wang Z, Luo L, Ren C (2012) Integrating AVHRR and MODIS data to monitor NDVI changes and their relationships with climatic parameters in Northeast China. Int J Appl Earth Obs Geoinf 18(1):528–536

Martre P, Wallach D, Asseng S, Ewert F, Jones JW, Rötter RP, Boote KJ, Ruane AC, Thorburn PJ, Cammarano D, Hatfield JL, Rosenzweig C, Aggarwal PK, Angulo C, Basso B, Bertuzzi P, Biernath C, Brisson N, Challinor AJ, Doltra J, Gayler S, Goldberg R, Grant RF, Heng L, Hooker J, Hunt LA, Ingwersen J, Izaurralde RC, Kersebaum KC, Müller C, Kumar SN, Nendel C, O'leary G, Olesen JE, Osborne TM, Palosuo T, Priesack E, Ripoche D, Semenov MA, Shcherbak I, Steduto P, Stöckle CO, Stratonovitch P, Streck T, Supit I, Tao F, Travasso M, Waha K, White JW, Wolf J (2015) Multimodel ensembles of wheat growth: many models are better than one. Glob Chang Biol 21:911–925

Meehl G, Covey C, Delworth T, Latif M, McAvaney B, Mitchell J, Stouffer R, Taylor K (2007) The WCRP CMIP3 multimodel dataset: a new era in climatic change research. Bull Am Meteorol Soc 88: 1383–1394

Miao C, Duan Q, Sun Q, Li J (2013) Evaluation and application of bayesian multi-model estimation in temperature simulations. Prog Phys Geogr 37:727–744

Monteith J (1981) Evapotranspiration and surface temperature. Q J R Meteorol Soc 107:1–27

Pachauri R K, Allen M R, Barros V R, et al (2014) Climate change 2014: synthesis report. Contribution of Working Groups I, II aend III to the fifth assessment report of the Intergovernmental Panel on Climate Change. IPCC

Padgham J (2009) Agricultural development under a changing climate: opportunities and challenges for adaptation

Parry M, Rosenzweig C, Iglesias A, Livermore M, Fischer G (2004) Effects of climate change on global food production under SRES emissions and socio-economic scenarios. Glob Environ Chang 14:53–67

Pu L, Zhang S, Li F, Wang R, Yang J, Chang L (2018) Impact of farmland change on soybean production potential in recent 40 years: a case study in Western Jilin, China. Int J Environ Res Public Health 15(7):1522

Pu L, Zhang S, Yang J, Chang L, Bai S (2019) Spatio-temporal dynamics of maize potential yield and yield gaps in Northeast China from 1990 to 2015. Int J Environ Res Public Health 16(7):1211

Ruane A, Cecil L, Horton R, Gordónd R, McCollume R, Browne D, Killough B, Goldberg R, Greeley A, Rosenzweig C (2013) Climate change impact uncertainties for maize in Panama: farm information, climate projections, and yield sensitivities. Agric For Meteorol 170:132–145

Scherm H (2004) Climate change: can we predict the impacts on plant pathology and pest management? Can J Plant Pathol 26:267–273

Schmidhuber J, Tubiello F (2007) Global food security under climate change. Proc Natl Acad Sci U S A 104:19703–19708

Shortridge A, Messina J (2011) Spatial structure and landscape associations of SRTM error. Remote Sens Environ 115:1576–1587

Smith M (1992) Expert Consulation on revision of FAO methodologies for crop water requirements. Nutr Rev 43(2):49–51

Solomon S, Qin D, Manning M et al (2007) Climate Change 2007: The Physical Science Basis; Contribution of working group I to the Fourth Assessment Report of the Intergovernmental Panel on Climate Change-Summary for Policymakers. IPCC Working Groups Reports

Sun X, Ren B, Zhuo Z, Gao C, Zhou G (2006) Faunal composition of grasshopper in different habitats of Northeast China. Chinese Journal of Ecology 25(3):286–289

Tan J, Li Z, Yang P et al (2014) Spatiotemporal changes of maize sown area and yield in Northeast China between 1980 and 2010 using spatial production allocation model. Acta Geograph Sin 69(3):353–364

Tao F, Zhang Z (2010) Adaptation of maize production to climate change in North China plain: quantify the relative contributions of adaptation options. Eur J Agron 33:103–116

Tao F, Yokozawa M, Zhang Z (2009) Modelling the impacts of weather and climate variability on crop productivity over a large area: a new process-based model development, optimization, and uncertainties analysis. Agric For Meteorol 149:831–850

Tebaldi C, Knutti R (2007) The use of the multi-model ensemble in probabilistic climate projections. Philos Trans R Soc A Math Phys Eng Sci 365:2053–2075

Williams J, Jones C, Kiniry J, Spanel D (1989) The EPIC crop growth model. Trans ASAE 32:497–511

Yuji M, Kiyoshi T, Hideo H, Yuzuru M (2009) Impact assessment of climate change on rice production in Asia in comprehensive consideration of process/parameter uncertainty in general circulation models. Agric Ecosyst Environ 131(3):281–291

Zhang T, Huang Y (2012) Impacts of climate change and inter-annual variability on cereal crops in China from 1980 to 2008. J Sci Food Agric 92:1643–1652

Zhou M, Wang H (2015) Potential impact of future climate change on crop yield in northeastern China. Adv Atmos Sci 32(7):889–897